

Wave Energy Dissipation over Porous Media

S.R. Pudjaprasetya, I. Magdalena

Industrial & Financial Mathematics Research Group
Fac. of Mathematics and Natural Sciences
Institut Teknologi Bandung, Indonesia
Jalan Ganesha 10, Bandung, West Java, Indonesia
ikha.magdalena@yahoo.com

Copyright © 2013 S. R. Pudjaprasetya and I. Magdalena. This is an open access article distributed under the Creative Commons Attribution License, which permits unrestricted use, distribution, and reproduction in any medium, provided the original work is properly cited.

Abstract

This paper study the effectiveness of a submerged porous media in dissipating wave energy of an incoming wave. We assume the porous breakwater is above an impermeable seabed. From dispersion relation derived for this problem, we obtain wave transmission coefficient for a submerged porous breakwater. Analysis apply to dispersion relation shows that amplitude reduction depends on breakwater parameters such as, porosity, friction coefficient, relative structure height, and wave frequency. Further, we formulate an approximate and explicit equation for gravity waves over a porous media. The approximate equation is hyperbolic type written in variables surface elevation and discharge, with coefficients depend on the bottom, and porous layer. Numerical simulation of incoming waves over porous media shows dissipation of amplitude and energy. Numerical results show good agreement with experimental data.

Mathematics Subject Classification: 76S05, 81U30, 35L02

Keywords: Submerged porous media, dispersion relation, hyperbolic equation

1 Introduction

Study of wave propagation pass through a porous structure is of interest by coastal and ocean engineers. A porous structure allows water waves to transmit

through it with energy dissipation. Therefore, wave amplitude and wave energy are reduced. In reality, submerged porous breakwater are for instance, natural submerged barrier reefs or artificial reefs. Apart from their function to enhance a better marine environment, they also function as breakwater, and reduce beach erosion. This research may support the understanding of wave energy reduction due to interaction with submerged porous breakwater, and it may be useful for designing suitable dimension of artificial reefs.

Both emerged and submerged porous breakwater can function as efficient breakwaters, but their governing equations are different. Literatures for wave interaction with emerged porous breakwaters are for instance Sulisz [15], Liu & Jiangang Wen [10], Lynett et.al. [12], Liu et.al. [11]. They discuss interaction of monochromatic wave, or solitary wave with an emerged porous structure, using the non-linear porous flow model either Navier Stokes equations or Boussinesq equations. Sollitt and Cross [14] propose a potential theory to simplify the specific problem that the nonlinear drag in the porous structure was linearized by applying Lorentz's condition. Since then, the potential theory was adopted in many investigations, such as Madsen [9], Rojanakamthorn et.al. [13] and Dalrymple et. al. [3]. Chin-Piao Tsai et.al. [17] formulate an approximate linear equation for monochromatic waves over submerged permeable breakwater on a variable permeable bottom topography. Chao-Lung Ting et.al. [16] and Kazumasa [7] study wave propagation with current over permeable ripple beds and consider Bragg resonance phenomenon. Kobayashi [8] study wave transmission over rigid breakwater. Gu,Z. [5] study numerical modeling for wave energy dissipation within porous submerged breakwaters, and solve the equation using boundary integral element method.

In this paper effectiveness of a submerged permeable breakwater is studied. The permeable breakwater is considered above a seabed which is impermeable. From the full governing equation, dispersion relation for this problem is obtained. It turns out that the negative sign of imaginary part of the complex wave number are directly related to the wave energy dissipation due to submerged porous breakwater. Dimensional analysis applied to the dispersion relation can lead us to effectiveness of a submerged porous breakwater in reducing wave amplitude. Restriction to monochromatic waves lead us to an approximate equation of hyperbolic type. The approximate equation is written explicitly in variables surface elevation and horizontal flux. The characteristic of breakwater appear as coefficient (in complex form) of that equation. We solve the equation numerically using the Lax-Wendroff method. Several computations were conducted to find wave transmission coefficient for several geometry of submerged porous breakwater. The results show good agreement with experiments.

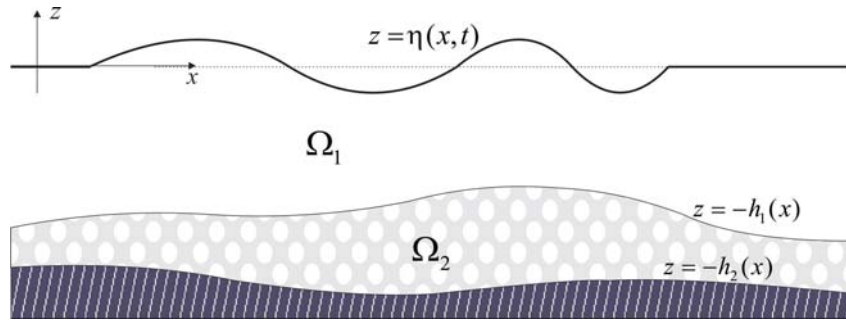


Figure 1: Definition sketch of submerged porous layer over an impermeable seabed.

2 Problem Formulations

The governing equation of the potential flow over a porous layer will be formulated below. Consider an upper region Ω_1 which is ideal fluid and a lower region Ω_2 which is ideal fluid in a porous media, see Figure 1. In region Ω_1 , the continuity equation and momentum equations are

$$\Delta\Phi = 0 \quad (1)$$

$$\Phi_t + \frac{1}{2}|\nabla\Phi|^2 + \frac{P_1}{\rho} + gz = 0 \quad (2)$$

respectively. Notation Φ is velocity potential, P_1 the dynamic pressure, ρ the density of water, g the gravitational acceleration. No particles flow through the surface leads to the kinematic boundary condition

$$\eta_t = -\Phi_x\eta_x + \Phi_z \quad \text{on} \quad z = \eta(x, t). \quad (3)$$

In region Ω_2 , the continuity equation and momentum equations are

$$\Delta\Psi = 0 \quad (4)$$

$$C^S\Psi_t + \frac{1}{2}|\nabla\Psi|^2 + \frac{P_2}{\rho} + gz + f^S\omega\Psi = 0, \quad (5)$$

respectively. Notation Ψ denotes velocity potential inside the porous medium. The term $f^S\omega\Psi$ represents the linearized friction factor, and C^S is the inertia coefficient of the flow in the porous medium. Impermeable boundary condition along the bottom $z = -h_2(x)$ reads

$$\Psi_x h_{2x} + \Psi_z = 0 \quad \text{on} \quad z = -h_2(x). \quad (6)$$

Along the interface fluid pressure is continuous $P_1 = P_2$, hence

$$\Phi_t + \frac{1}{2}|\nabla\Phi|^2 = C^S\Psi_t + \frac{1}{2}|\nabla\Psi|^2 + f^S\omega\Psi \quad \text{on} \quad z = -h_1(x). \quad (7)$$

Continuity equations (1,4) hold under the assumption that influx and outflux along the interface are the same

$$\Phi_x h_{1x} + \Phi_z = \varepsilon^S (\Psi_x h_{1x} + \Psi_z) \quad \text{on } z = -h_1(x), \quad (8)$$

with ε^S porosity of the porous medium. The linearized governing equations are

$$\Delta \Phi = 0, \quad \text{in } \Omega_1 \quad (9)$$

$$\Delta \Psi = 0, \quad \text{in } \Omega_2 \quad (10)$$

$$\Phi_t = -g\eta, \quad \text{on } z = 0, \quad (11)$$

$$\eta_t = \Phi_z, \quad \text{on } z = 0, \quad (12)$$

$$\Psi_z = 0, \quad \text{on } z = -h_2(x). \quad (13)$$

$$\Phi_t = C^S \Psi_t + f^S \omega \Psi, \quad \text{on } z = -h_1(x), \quad (14)$$

$$\Phi_z = \varepsilon^S \Psi_z, \quad \text{on } z = -h_1(x). \quad (15)$$

3 Dispersion Relation and Dimensional Analysis

In this section we will derive dispersion relation for the full linearized equations (9-15). Analysis of dispersion relation will show the main effect of porous media in wave evolution.

The next step is solving the full linear governing equations by separation of variables. Assuming $\Phi(x, z, t) = \frac{ig\eta(x,t)}{\omega} F(z)$, $\Psi(x, z, t) = \frac{ig\eta(x,t)}{\omega} F(z)$, where $\eta(x, t) = ae^{-i(kx-\omega t)}$, a is the wave amplitude, k is wave number, and ω is wave frequency, equations (9-12) reduce to

$$F_{zz} - k^2 F = 0$$

with boundary conditions $F(0) = 1$ and $F_z(0) = \frac{\omega^2}{g}$. The eigenfunction are $F(z) = \cosh kz + \frac{\omega^2}{gk} \sinh kz$, for any k .

Further, assuming $\Psi(x, z, t) = \frac{ig\eta(x,t)}{\omega} G(z)$, equations (10, 13) reduce to

$$G_{zz} - k^2 G = 0$$

with boundary conditions $G_z(-h_2) = 0$. Its solutions are $G(z) = C \cosh k(z + h_2)$. Using interface condition (15) in which $F_z(-h_1) = \varepsilon^S G_z(-h_1)$ we obtain

$$C = \frac{-\sinh kh_1 + \frac{\omega^2}{gk} \cosh kh_1}{\varepsilon^S \sinh k(h_2 - h_1)}. \quad (16)$$

Finally, from (14) we obtain the following dispersion relation

$$\frac{\omega^2}{gk} = \frac{\varepsilon^S \tanh k(h_2 - h_1) + \alpha^S \tanh kh_1}{\varepsilon^S \tanh kh_1 \tanh k(h_2 - h_1) + \alpha^S}, \quad (17)$$

with $\alpha^S = (C^S - if^S)$. We test the condition of no breakwater: (1) $h_1 = h_2$ or (2) $\varepsilon^S = 1$, $f^S = 0$ and $C^S = 1$. Each of this limiting case will yield the well-known dispersion relation for gravity wave: $\frac{\omega^2}{gk} = \tanh kh_2$, as we expect. Similar derivation of dispersion relation for infinite depth can be obtained in Dean & Dalrymple [4].

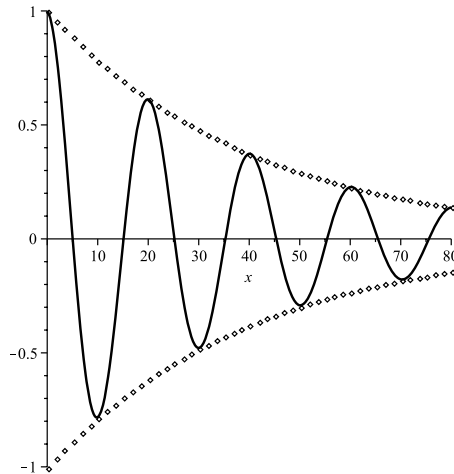


Figure 2: The curve $\eta(x, t) = \exp^{-i(kx - \omega t)}$ with $k = 0.3117600956 - 0.02450305720 I$ (solid line) and its envelope (dotted line) $K_T = |\eta(x, t)|$.

Taking parameter values $\omega = 1$, $h_1 = 1$, $h_2 = 1.7$, $\varepsilon = 0.4$, $C^S = 0.4$, $f^S = 1.5$, dispersion relation (17) will give us a complex value wave number $k = 0.3117600956 - 0.02450305720 I$. A monochromatic wave $\exp^{-i(kx - \omega t)}$ with negative imaginary part $\Im(k)$ will undergo amplitude reduction, see Figure 2. Let $K_T = |\eta(x, t)| = \exp \Im(k)x$, the term K_T denotes amplitude reduction of incident wave as a function of x , the horizontal length of a submerged porous breakwater. It also denotes the ratio between wave transmission amplitude and incident wave amplitude, which is usually called wave transmission coefficient.

It is clear that the profile of wave transmission coefficient depends strongly on the complex wave number k , and hence on the dispersion relation (17). Parameters involve in (17) are wave frequency ω , gravitational constant g , porosity ε^S , C^S , f^S , h_1 and the structure depth $h_2 - h_1$. Armono and Hall [1] study wave transmission coefficient with respect to breakwater parameter such

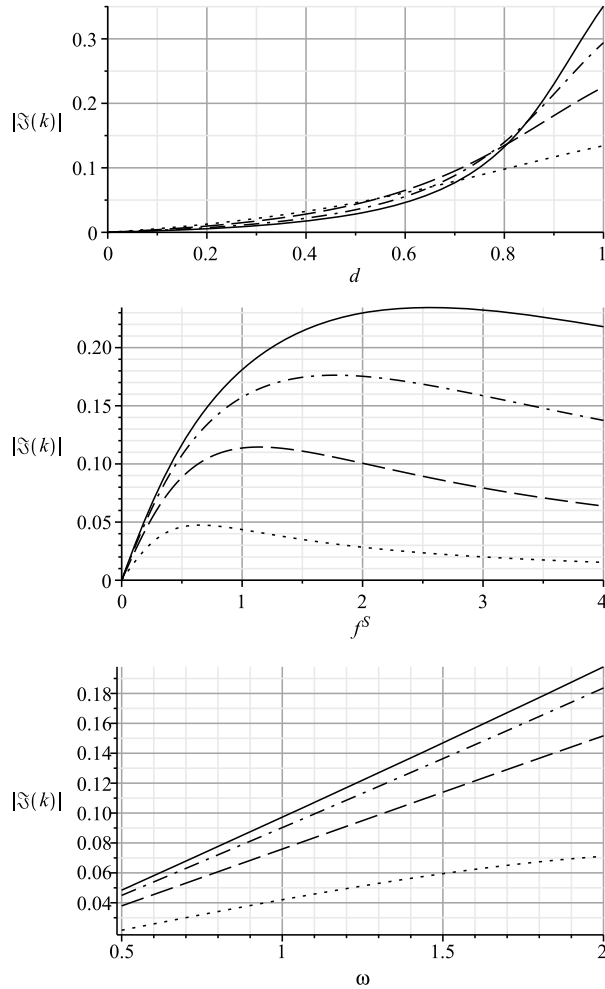


Figure 3: (Top) Curves of $|\Im(k)|$ w.r.t. $d = (h_2 - h_1)/h_2$ for $f^S=0.5$ (dot), 1(dash), 1.5(dashdot), 2(solid). (Middle) Curves of $|\Im(k)|$ w.r.t. f^S for $d =.5$ (dot), $.75$ (dash), $.85$ (dashdot), $.9$ (solid). (Bottom) Curves of $|\Im(k)|$ w.r.t. ω for $d =.5$ (dot), $.75$ (dash), $.85$ (dashdot), $.9$ (solid).

as, porosity, relative structure height, wave frequency and other parameters. Here, we apply dimensional analysis in order to study the dependence of $\Im(k)$ on those parameters. In total there are 6 parameters and 2 variables: $\Re(k)$ and $\Im(k)$, and there are two dimensions $[L], [T]$. Hence, there are 6 non-dimensional variables. Three of them are ε^S, C^S, f^S . The other three non-dimensional variables we choose $r = \omega^2 h_2/g, \kappa = kh_2$, and $d = (h_2 - h_1)/h_2$. We focus on the magnitude of $|\Im(k)|$ with respect to the non-dimensional variables d (relative reefball height), f^S , and r (normalized frequency). Approximating

$\tanh x \approx x$ dispersion relation (17) becomes

$$\omega^2 \varepsilon^S k^2 h_1 (h_2 - h_1) + \alpha^S \omega^2 = g \varepsilon^S k^2 (h_2 - h_1) + g \alpha^S k^2 h_1$$

By multiplying with h_2/g and writing in terms of r, κ, d will yield

$$\kappa^2 (\varepsilon^S d + \alpha^S (1 - d) - \varepsilon^S r (1 - d) d) = \alpha^S r. \tag{18}$$

Using (18) we can directly plot a curve of $|\Im(k)| = |\Im(\kappa)|/h_2$ with respect to variables d, f^S and r . For all computations follows we take $\varepsilon = 0.4, C^S = 0.4, h_2 = 1.7, g = 9.8$. Figure 3 (top) shows a curve of $|\Im(k)|$ with respect to d using $\omega = 1$ for several values of f^S . It is clear from the figure that a larger relative reefball height d yields a larger value of $|\Im(k)|$, and hence more damping. The curve of $|\Im(k)|$ with respect to f^S for several values of d , with $\omega = 1$ is given in Figure 3 (middle). We observe that value of f^S that yield a maximum $|\Im(k)|$ changes with d . Finally, Figure 3 (bottom) is the curve of $|\Im(k)|$ with respect to ω for several values of d , with $f^S = 1.5$. Clearly, the effect of each parameter in the wave attenuation can be analyzed directly through $|\Im(k)|$, so this analysis may useful for designing a suitable dimension of porous breakwater.

4 The Mild Slope Equation

In this section we will formulate an approximate evolution equation that holds for slowly varying $h_1(x)$ and $h_2(x)$. The following is the standard procedure of mild slope equation derivation: multiply (9) with $F(z)$ and integrate from $z = -h_1$ to $z = 0$, and multiply (10) with $G(z)$ and integrate from $z = -h_2$ to $z = -h_1$, adding both yields

$$\int_{-h_1}^0 \Delta \Phi F(z) dz + \varepsilon^S \alpha^S \int_{-h_2}^{-h_1} \Delta \Psi G(z) dz = 0.$$

Applying partial integration yields

$$\int_{-h_1}^0 (\Phi_{xx} F(z) - \Phi_z F_z) dz + \Phi_z F|_{-h_1} + \varepsilon^S \alpha^S \int_{-h_2}^{-h_1} (\Psi_{xx} G(z) - \Psi_z G_z) dz + \Psi_z G|_{-h_2}^{-h_1} = 0.$$

Further we assume $\Phi(x, z, t) = \bar{\Phi}(x, t) F(z)$, $\Psi(x, z, t) = \bar{\Phi}(x, t) G(z)$, and the above equation becomes

$$\int_{-h_1}^0 (\bar{\Phi}_{xx} F^2 - \bar{\Phi} F_z^2) dz + \Phi_z F|_{-h_1} + \varepsilon^S \left\{ \alpha^S \int_{-h_2}^{-h_1} (\bar{\Phi}_{xx}^S G^2 - \bar{\Phi}^S G_z^2) dz + \Psi_z G|_{-h_2}^{-h_1} \right\} = 0.$$

By using boundary condition (12) and neglecting higher order terms, the equation above reduces to

$$\eta_t + \partial_x \left(\left\{ \int_{-h_1}^0 F^2 dz + \varepsilon^S \alpha^S \int_{-h_2}^{-h_1} G^2 dz \right\} \bar{\Phi}_x \right) - \left(\int_{-h_1}^0 F_z^2 dz + \varepsilon^S \alpha^S \int_{-h_2}^{-h_1} G_z^2 dz \right) \bar{\Phi} = 0 \tag{19}$$

By substituting $F(z), G(z)$ obtained previously, equation (19) becomes

$$\eta_t + \partial_x \left(\frac{nc^2}{g} \bar{\Phi}_x \right) - \frac{\omega^2}{g} (1 - n) \bar{\Phi} = 0. \tag{20}$$

From the boundary condition (12) we have the relation $\bar{\Phi} = \frac{g}{\omega^2} \eta_t$, so we can rewrite (20) as

$$\eta_t + \frac{1}{n} \partial_x \left(\frac{nc^2}{g} \bar{\Phi}_x \right) = 0, \tag{21}$$

with

$$c^2 = \left(\frac{\omega}{k} \right)^2 = \frac{g \varepsilon^S \tanh k(h_2 - h_1) + \alpha^S \tanh kh_1}{k \varepsilon^S \tanh kh_1 \tanh k(h_2 - h_1) + \alpha^S}, \tag{22}$$

$$n = \frac{1}{2} + \frac{\kappa d \varepsilon^S \alpha^S + \kappa \left((\alpha^S \cosh \kappa d)^2 - (\varepsilon^S \sinh \kappa d)^2 \right)}{2[SH][CH]}, \tag{23}$$

where

$$[SH] = \varepsilon^S \cosh kh_1 \sinh \kappa d + \alpha^S \sinh kh_1 \cosh \kappa d$$

$$[CH] = \varepsilon^S \sinh kh_1 \sinh \kappa d + \alpha^S \cosh kh_1 \cosh \kappa d.$$

The equation (21) should be accompanied with the dynamic free surface boundary condition (11). Rewriting (21) and (11) in terms of η and a flux like variable $q \equiv \frac{c^2}{g} \bar{\Phi}_x$, we get the following simple hyperbolic equations

$$\begin{cases} \eta_t + \frac{1}{n} (nq)_x = 0 \\ q_t + c^2 \eta_x = 0, \end{cases} \tag{24}$$

The evolution equation (24) is of hyperbolic type, with coefficients n and c^2 depend on the geometry of breakwater and topographies $h_1(x), h_2(x)$, and porous breakwater parameters: C^S, f^S, ε^S . Note that if k is a complex number, then c^2 as given in (22) is also complex. When $h_1(x)$ and $h_2(x)$ are constant, n is also constant, and the first equation of (24) becomes $\eta_t + q_x = 0$. Condition of no breakwater: (1) $h_1 = h_2$ or (2) $\varepsilon^S = 1, f^S = 0, C^S = 1$. In both cases, the linear propagation speed reduces to $c^2 = g \tanh kh_2/k$ as we expect. Wiryanto[18] consider the same problem by implementing Boussinesq assumption and in first order approximation obtain similar hyperbolic equation in variable surface elevation η and averaged horizontal velocity Φ_x , with the effect of porous structure appears as the forcing term.

5 Numerical Simulation

The Lax-Wendroff method is a finite difference method with accuracy $\mathcal{O}(\Delta t^2, \Delta x^2)$, it is available in many textbook, see for instance [6]. Implementation of Lax

Wendroff method to (24) will yield the following discretized equations

$$\eta_j^{m+1} = \eta_j^m - \frac{1}{n_j} \frac{\Delta t}{2\Delta x} (nq|_{j+1}^m - nq|_{j-1}^m) + \frac{c^2}{n_j} \frac{\Delta t^2}{2\Delta x^2} (n\eta|_{j+1}^m - 2n\eta|_j^m + n\eta|_{j-1}^m) \quad (25)$$

$$q_j^{m+1} = q_j^m - c^2 \frac{\Delta t}{2\Delta x} (\eta_{j+1}^m - \eta_{j-1}^m) + c^2 \frac{\Delta t^2}{2\Delta x^2} (q_{j+1}^m - 2q_j^m + q_{j-1}^m) \quad (26)$$

The Von-Neumann stability condition is $|c| \frac{\Delta t}{\Delta x} \leq 1$. For simulation of an incoming monochromatic wave passing over a submerged porous breakwater, we take a zero initial condition $\eta(x, 0) = q(x, 0) = 0$ and the left influx monochromatic wave of amplitude a :

$$\begin{cases} \eta(0, t) = -ai e^{i\omega t} \\ q(0, t) = c\eta(0, t). \end{cases} \quad (27)$$

Along the right boundary, we apply the Forward Time Backward Space (FTBS) method that represents a right absorbing boundary. We test the scheme for no porous condition: $h_1 = h_2$ and take $c^2 \approx gh_2$, equation (24) reduces to the simple wave equation: $\eta_t + q_x = 0$, $q_t + gh_2\eta_x = 0$. Numerical simulation for h_2 constant, using zero initial condition and boundary condition (27) will yield a monochromatic wave travels undisturbed in shape.

For simulations of wave evolution in the area with submerged porous media, we use the following steps. (1) Solve (17) for k , for a specific choice of parameters ε^S, C^S, f^S and topographies $h_1(x), h_2(x)$, (2) with this value of k we compute c^2 and n from (22) and (23), respectively. Note that c^2 is a complex number. (3) Implement the Lax-Wendroff discretization (25,26). For computations we use $\Delta x = 0.1$ and in order to prevent numerical diffusion error we take $\Delta t = \Delta x/|c|$. We note here that if we compute $\lim_{t \rightarrow \infty} \sqrt{\Re(\eta)^2 + \Im(\eta)^2}$ and plot it with respect to x , we obtain the same wave transmission coefficient curve as in Figure 2. Hence, the numerical computation confirms the analytical result of wave transmission coefficient K_T .

Numerical simulation of an incoming monochromatic wave passing over a submerged porous breakwater is given in Figure 4 (top). For this computation, we use the linear shallow water equation in free water areas on the downstream and upstream sides of porous breakwater, also continuity of η and q on the left and right interfaces. For computation we use the same set of parameters: $\omega = 1$, $h_1 = 1$, $h_2 = 1.7$, $\varepsilon^S = 0.4$, $C^S = 0.4$, $f^S = 1.5$ from which dispersion relation (17) yield $k = 0.3117600956 - 0.02450305720 I$. It clearly shows that the wave amplitude is reduced. We plot the wave energy, defined as $\Re(\eta)^2 + \Im(\eta)^2$ in Figure 4 (bottom), the result shows reduction of wave energy.

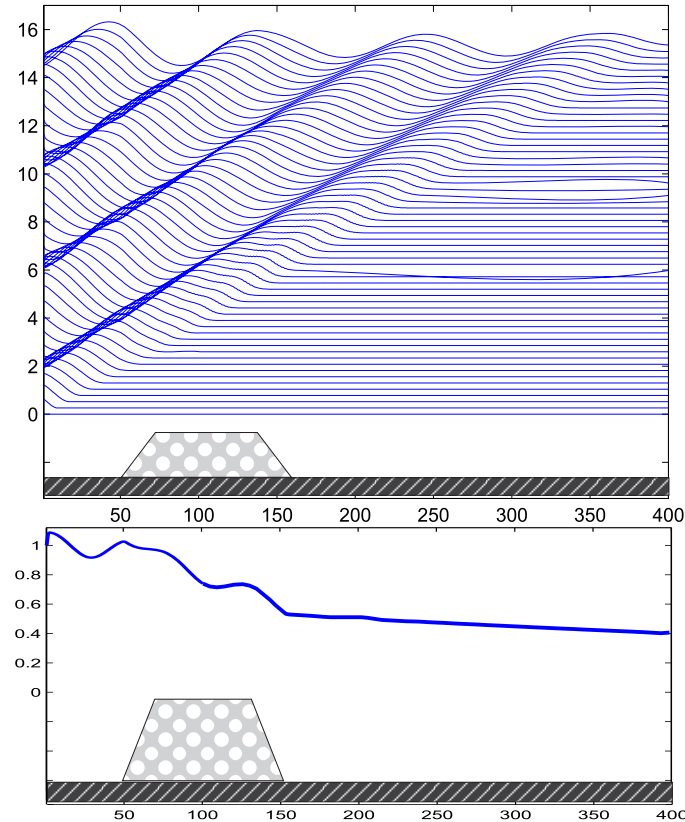


Figure 4: (Top) Amplitude of incoming monochromatic wave reduces after passing a submerged porous breakwater. (Below) Wave energy reduces after passing a submerged porous breakwater. The height of trapezoid porous breakwater is not to scale.

5.1 Comparison with Experiment

Experiments of amplitude reduction due to submerged porous breakwater were carried out in a wave tank 8 m length and 0.3 m width, and 0.5 m height. A model of an absorbed beach is set on the right side of the wave flume. A breakwater model is located on the center of the wave tank. It is made from round stones of diameter 0.01 m densely packed in a box casing made from wire. The porosity of the model is set $\varepsilon^S = 0.46$. Experiments use water depth $h_2 = 0.15$ m. Wave amplitude at different positions along the wave tank are measured. From this data we compute wave transmission coefficient K_T experiment. Comparison with K_T from numerical computations shows good agreement.

Table 1: Wave transmission coefficients obtained from experiment and numeric.

L_b	frequency (rpm)	Wave transmission coefficient K_T			
		d=0.078 m		d=0.106 m	
		experiment	numeric	experiment	numeric
20.59 cm	25	82.97%	82.54%	66.42%	67.37%
	30	87.04%	87.73%	70.11%	73.12%
	35	97.62%	98.03%	83.33%	84.57%
42.29 cm	25	68.58%	67.91%	45.37%	46.15%
	30	77.62%	78.63%	53.26%	55.23%
	35	90.75%	95.48%	39.78%	75.51%

6 Conclusions

Analysis of dispersion relation can give us a clear picture of the dissipative effect of a submerged porous breakwater with certain specification. The effect of each parameter can be analyzed directly so that it may useful for designing suitable dimension of porous breakwater. Moreover, the mild slope equation for wave over a submerged porous media is of hyperbolic type, with a complex value coefficient. The Lax-Wendroff method is a stable method for simulating amplitude reduction of monochromatic wave past over a submerged porous layer. Wave amplitude and wave energy are reduced. This amplitude reduction is confirmed with data from experiment.

Acknowledgements. This research is supported by grant 020/ K01.7.1.1/FMIPA-IMHERE ITB/2010 and Riset KK 2012 413/1.1.C01/PL/2012. The authors would like to thank L.H. Wiryanto for financial support of the experiment and useful discussions.

References

- [1] Armono, H.D, Hall, K.R., Wave transmission on submerged breakwater made of hollow hemispherical shape artificial reefs, *Proceeding of The 1st Coastal, Estuary and Offshore Engineering Speciality Conference*, (2003),CSC-185-1:10.
- [2] Fernando, H.J.S., Samarawickrama, S.P., Balasubramanian, S., Hettiarachchi, S.S.L., Voropayev, S., Effects of porous barriers such as coral reefs on coastal wave propagation, *Journal of Hydro-environment Research*, **1** (2008), 187-194.

- [3] Dalrymple, R.A., Losada, M.A., Martin, P.A., Reflection and transmission from porous structures under oblique wave attack, *Journal of Fluid Mechanics*, **224**(1991) , 625644.
- [4] Dean R.G., Dalrymple R.A., *Water Wave Mechanics for Engineers and Scientists*, World Scientific, 1991.
- [5] Gu,Z. and Wang,H., Numerical Modeling for Wave Energy Dissipation within Porous Submerged Breakwaters of Irregular Cross Section, *Coastal Engineering*, **90**(1992) ,1189-1198.
- [6] Hoffman, Joe. , *Numerical Methods for Engineers and Scientist 2nd edition*, Mc.Graw-Hill.inc. New York, 2001.
- [7] Kazumasa Mizumura, Free Surface Flow over Permeable Wavy Bed, *Journal of Hydraulic Engineering*, Vol. 124, No. **9**(1998), 955-962.
- [8] Kobayashi,N. and Wurjanto., Wave Transmission over Submerged Breakwaters, *Journal of Waterways, Port, Coastal Engineering*, ASCE, **115**(1989), No.5, 662-680.
- [9] Madsen, O. S., Wave transmission through porous structures. *Journal of Waterways, Harbors, Coastal Engineering Division*, ASCE, **100**(1974), 169188.
- [10] Liu, P.L.F. & Jiangang Wen., Nonlinear diffusive surface waves in porous media. *Journal Fluid Mech.*, **347**(1997), 119-139.
- [11] Liu, P.L.F., Lin, P., Chang, K.A., Tsutomu Sakakiyama., Numerical modeling of wave interaction with porous structures, *Journal of Waterway, Port, Coastal, and Ocean Engineering*, (1999) ,322-330, Nov-Dec.
- [12] Lynett, P.J. , Liu, P.L.F., Losada, I.J., Vidal, C., Solitary wave interaction with porous breakwaters, *Journal of Waterway, Port, Coastal, and Ocean Engineering*, (2000),314-322.
- [13] Rojanakamthorn, S., Isobe, M., Watanabe, A., A mathematical model of wave transformation over a submerged breakwater, *Coastal Engineering in Japan*, **31 (2)** (1989), 209234.
- [14] Sollitt, C.K., Cross, R.H., Long-wave transmission through porous breakwaters, *Proc. 13th Coastal Eng. Conf., ASCE*, New York, Vol. **3**(1972), 1827-1846.
- [15] Sulisz, W., Wave reflection and transmission at permeable breakwaters of arbitrary cross-section,*Coastal Engineering*, **9**(1985), 371–386.

- [16] Ting, C.L., Lin, M.C., Kuo, C.L., Bragg scattering of surface waves over permeable rippled beds with current, *Physics of Fluids*, Vol. 12, No. **6**(2000), 1382-1388.
- [17] Tsai, C.P., Chen, H.B., Lee, F.C., Wave Transformation Over Submerged Permeable Breakwater on Porous Bottom, *Ocean Engineering*, **33**(2006), 1623-1643.
- [18] Wiryanto, L.H., Wave propagation passing over a submerged porous breakwater, in *J. Eng. Mathematics*, **70**(2011), 129-136.

Received: March 14, 2013